FORMATION AND STEERING MECHANISMS OF TORNADO CYCLONES AND ASSOCIATED HOOK ECHOES[1]

TETSUYA FUJITA

The University of Chicago, Chicago, Ill.

ABSTRACT

An attempt is made to explain the mechanism of a hook-echo formation on the southwestern edge of an eastward-moving cumulonimbus cell. The conditions necessary for originating a hook-echo circulation through this proposed mechanism are: significant absolute vorticity within the subcloud layer, intense updraft to bring the low-level moist air into the cloud, and a vertical wind shear which steers the cumulonimbus cell with a velocity which is considerably different from that of the low-level winds. The Magnus effect involving the steering current and the spiraling updraft is considered to be the force which directs the hook-echo circulation at low levels toward the southwestern edge of the major thunderstorm cell. A kinematic diagram with the absolute tangential speed and the radius of the cyclone as coordinates is also presented, as well as some speculation on the conservation of absolute circulation and absolute vorticity.

1. INTRODUCTION

Recent developments in weather radar make it possible to detect tornado cyclones when they are associated with the familiar shape of a so-called hook echo. A hook echo does not always accompany tornadoes, although the probability of observing tornadoes in the vicinity of the path of a hook echo is extremely high compared with that of an ordinary thunderstorm echo. A large percentage of reported tornadoes may not be related to tornado cyclones, either because they just form out of unknown cloud structures or because no radar was available to verify the mother circulations.

In view of the importance of the role of hook echoes in forecasting tornadoes, mechanisms of hook-echo formations were proposed by several meteorologists, notably Fulks [8], who attempted to explain the frequent observations of hook echoes near the southwestern edge of a mature thunderstorm cell moving eastward. In his model a large convective tower extending into the levels of strong vertical wind shear acts favorably in producing cyclonic and anticyclonic flows at the opposite ends of the tower, of which the cyclonic flow to the southwest gives rise to the hook-echo development.

Since then a number of PPI-picture sequences taken with high elevation angles became available making it possible to examine the vertical extent of the hook echo in relation to the intense echo usually observed on the forward left side of the hook.

The tornado cyclone postulated by Brooks [2] is characterized by an overall horizontal dimension of about 10 mi. If a well-defined circulation exists around the center, it would appear as either a hole in the echo or a hook echo of the dimensions under discussion.

Because of the unusually unfavorable weather conditions for taking pictures, there exist only a limited number of photographs showing the entire rotating cloud. The Fargo storm of June 20, 1957, photographed by a large number of local citizens and studied by Fujita [4], is probably the best documented terrestrial photography of a tornado-cyclone cloud. Figure 1 shows the remarkable circulation at the base of this rotating cloud, which produced five tornadoes, one after another.

During the 1961 operation of the National Severe Storms Project based at Oklahoma City, Okla., the U.S. Weather Bureau's instrumented aircraft (B-57, DC-6B, and B-26) made a successful attempt to collect multi-level meteorological data of an isolated cumulonimbus on April 21, 1961 (fig. 2). The storm originated as three small towers shortly after 1500 CST and grew into a cumu-

FIGURE 1.—A rotating cloud pictured at Fargo, N. Dak. on June 20, 1957. Five tornadoes were produced by this cloud causing extensive damage in Fargo and nearby communities. Diameter of circulation included in the picture: 5 mi. Distance to the circulation center: 7 mi. Azimuth of the center: 249°. (Courtesy Stenerson.)

lonimbus with a 50-mi.-long anvil after about one hour. Further details of this cloud appear in the report by Fujita and Arnold [6]. A vorticity of about 100×10^{-5} sec.$^{-1}$ was computed within the subcloud layer at the time of this picture. The whole tower in the foreground was rotating at an unknown rate while moving eastward. In fact, a tornado was reported 25 min. later from a town some 10 mi. to the east. Clouds with such rotational characteristics are expected to give rise to the development of tornadoes.

2. TORNADO CYCLONES AS OBSERVED BY RADAR

Because of its long range and rapid scan capabilities that permit short-interval time-lapse photographs, radar provides more opportunities to detect rotating clouds than terrestrial and aerial photography combined.

Since the first radar pictures of a hook echo associated with tornadoes were taken and investigated by Stout and Huff [12], numerous hook echoes and those with rotational characteristics have been obtained. It should be noted, however, that a hook echo, even though it is located within the detectable range, cannot always be seen on the scope unless gain setting, pulse length, beam width, and antenna elevation are properly combined for the detection of the relatively small circulation inside a cloud. Penn, Pierce, and McGuire [11] demonstrated that the hook echo associated with the Worcester tornado appeared quite different in the radar pictures taken by the Massachusetts Institute of Technology (Cambridge) and by Project Lincoln (Lexington).

On May 26, 1963, during the operation of the National Severe Storms Project, the WSR-57 radar at the Weather Radar Laboratory[2] in Norman, Okla. obtained a series

of pictures involving the formation and subsequent development of several hook echoes in central Oklahoma (fig. 3).

A series of gain-step pictures taken with a zero-degree elevation angle revealed a small hole in the middle of an echo in a reduced-gain picture. The hole, located 45 n. mi. to the north-northwest of the radar, would not have been recognized if a proper gain setting had not been employed. This hole, which is indicated by an arrow with number 2 in the step-4 picture, changed into a hook echo some 20 min. later.

Radar observers and meteorologists have noted that a hook echo is usually located near the west-southwestern edge of the major thunderstorm cell traveling eastward. For a major cell traveling in a different direction, the hook echo forms in the same relative location with respect to the major cell. These relative positions of the major cell and the hook echo are readily detected when one observes the storm with a low elevation angle. It is customary for the radar operator to bring the beam to a low elevation angle in order to observe a distinct hook echo on a PPI scope. When the elevation angle is raised a few degrees, either the hook or the hole in the echo does not remain near the west-southwestern edge of the major cell, but tends to disappear into the cell, thus making it very difficult to identify the vortex in the cloud. This fact implies a tilt of the circulation axis.

With the use of a series of antenna-tilt step pictures of dual hook echoes of May 26, 1963, as shown in figure 4, the positions of the circulation center were plotted in the pictures with elevation angles up to 18°. The time interval between the two zero-tilt photographs was only 5 min. (1621 to 1626 CST). This makes it possible to justify a linear interpolation of the positions of the hook echo during this short period. Open circles in the figure denote the positions of two hook echoes at low
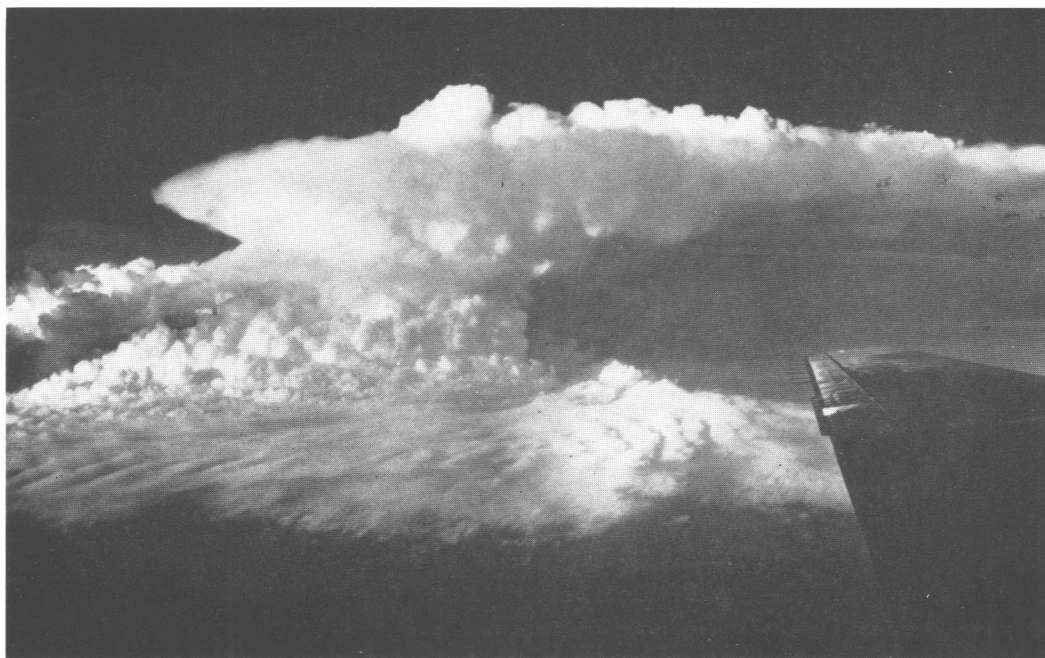
FIGURE 2.—View of a cumulonimbus cloud accompanied by a rotating cloud tower near the west-southwestern edge of the main cloud mass. Time: 1750 CST, April 21, 1961. Flight altitude: 20,000 ft. Distance to the rotating tower: 10 mi. (Photographed by Fujita from Weather Bureau's DC–6B.)

levels near the ground. It is seen that the major cells photographed with zero-degree tilt changed little in shape and moved slightly east-southeastward. A rather striking feature in this figure is the location of the hook-echo circulation near the ground, which coincides with the center of the major cell between the 30,000- and 40,000-ft. levels. The figure includes the intersections of the scan cone of the beam and the horizontal planes at 1,000-ft. intervals. The axis of the hook-echo circulation does not usually tilt more than 20° from the local vertical, thus resulting in no more than a 2-mi. shift in the position of the circulation centers at levels of a few thousand and 30,000 ft.
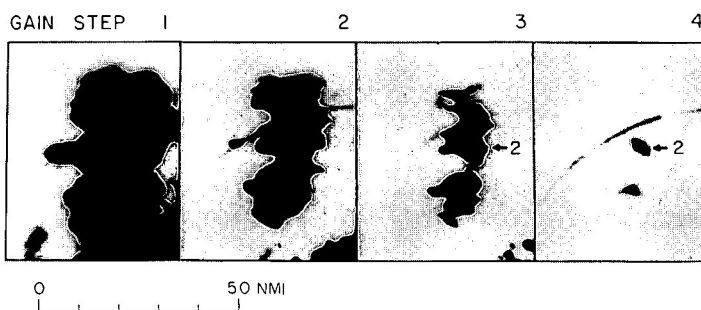

FIGURE 3.—A hole in a large solid echo appearing in the gain-step picture. The hole is seen in the step-4 picture only. The tilt of antenna for all gain-steps was zero degree. WSR–57 radar at NSSL, Norman, Okla., 1540 CST, May 26, 1963.
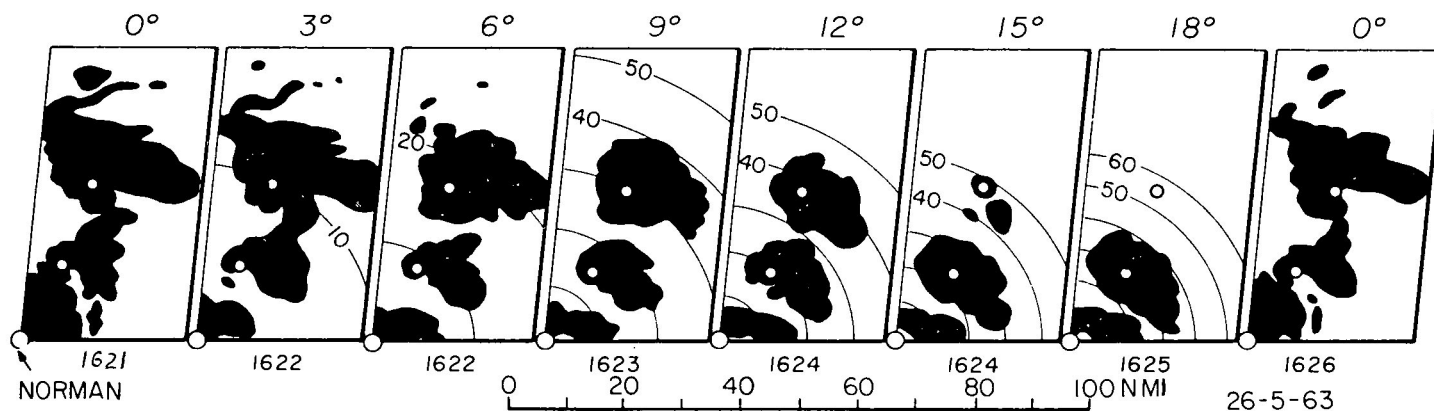

FIGURE 4.—Position of the hook echoes (open circles) at low levels plotted with the echo boundaries on PPI photographs obtained by tilting the antenna up to 18° at 3° increments. The positions of the open circles were interpolated from the first and last pictures obtained with 0° antenna tilt. The concentric circles centered at Norman denote the line of intersection between the scan cone and the horizontal planes with heights at 1,000-ft. intervals above radar.
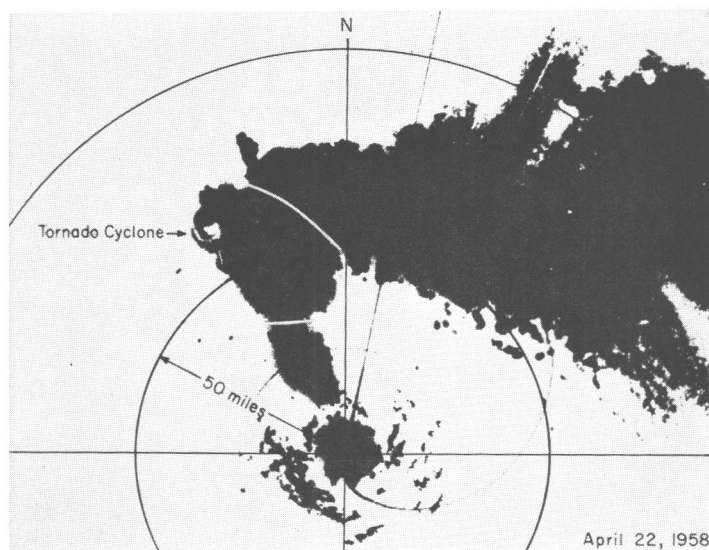
FIGURE 5.—A hook echo photographed by Texas A and M radar at 1815 CST, April 22, 1958. (Courtesy S. G. Bigler.) Reduced-gain pictures show that a major cell associated with the hook echo extends only within the area separated by the two white lines. The major echo is located in the left-forward sector of the hook echo which is moving toward the south-southeast at 37 kt.

FIGURE 7.—CAPPI presentation of cloud-top and cloud-base topography of April 22, 1958, storm photographed by Texas A and M radar. The eye of the tornado cyclone at 30,000 ft. is shown by the small solid circle. It was moving toward the 150° direction at 37 kt. In the upper chart the spreading of the cloud top estimated from the echo contour is shown by the arrows. Two curved arrows in the lower chart represent the estimated hook-echo circulation at low levels.

At about 50,000 ft., intersected with 15° elevation, the position of the surface circulation center of the northern cloud coincides with one of the three tall convective towers which are probably overshooting the cirrus deck. If photographed from a high-flying aircraft, these echoes between 40,000 and 50,000 ft. would appear as such overshooting turret tops as are shown in figure 2.

In order to depict the three-dimensional feature of such a cloud, it is necessary to construct CAPPI charts of the echo at various altitudes. The method of CAPPI construction developed by Marshall [10] was used in synthesizing the pictures taken with various elevation angles.

Even though the picture series of the May 26, 1963, storm presented an excellent example of multi-elevation angle views of the rotating cloud, a tornado cyclone case reported by Bigler [1] was used in constructing CAPPI charts. The PPI and RHI pictures are shown in figures 5 and 6, respectively. The eye was moving toward the
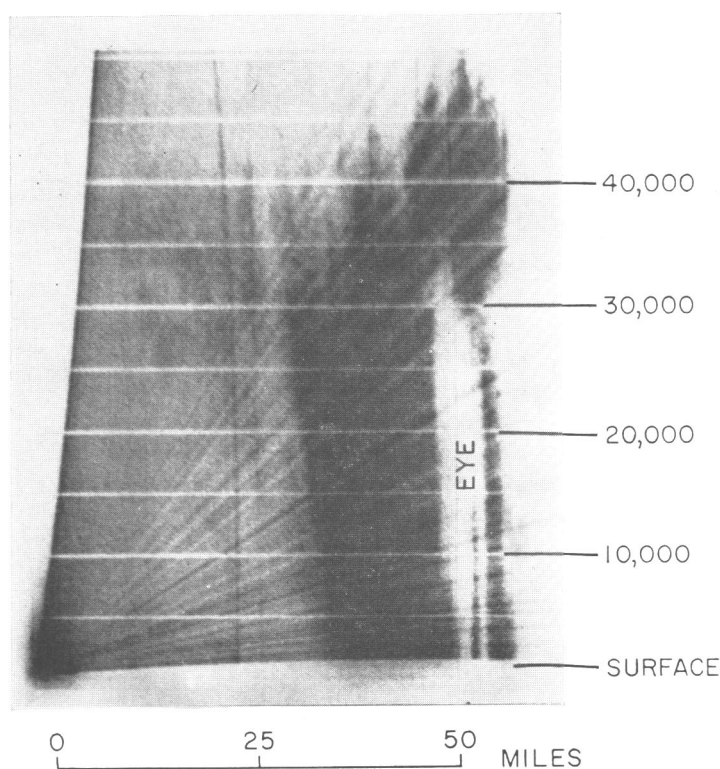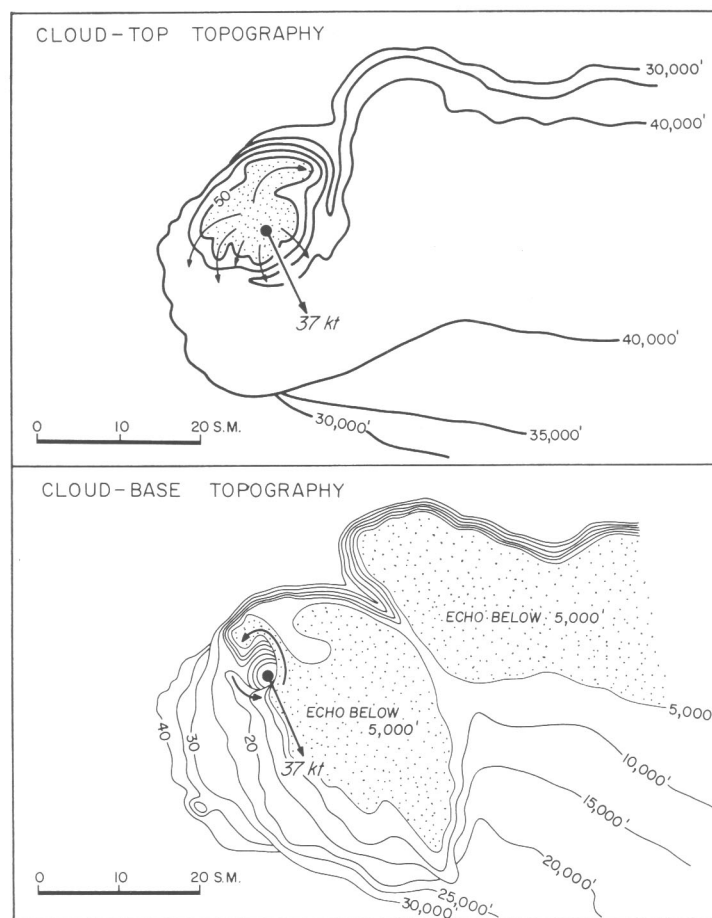

FIGURE 6.—The eye of the April 22, 1958, tornado cyclone photographed at 1827 CST by Texas A and M radar. (Courtesy S. G. Bigler.) When scanned with extremely low elevation angles, a so-called hook echo appears on the PPI scope. Even though a hook echo represents the low-level circulation, the vortex as a whole extends beyond 30,000 ft.
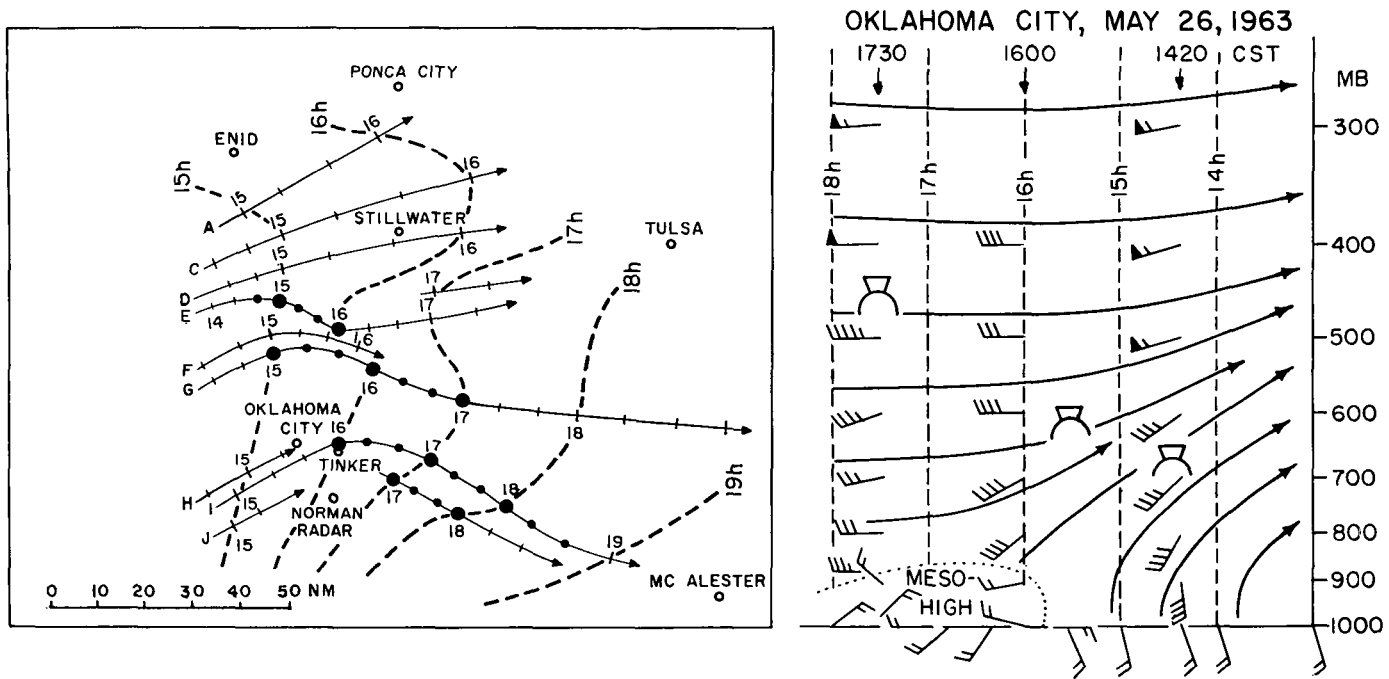
FIGURE 8.—(Left) Trajectories of echoes as identified by the letters A, C, D, . . . J, which appeared between 1400 and 1500 CST, May 26, 1963. Black circles represent positions of the cloud which showed definite signs of cyclonic rotation, and the short cross lines on each echo track represent non-rotating clouds. The numbers beside the echo tracks designate the hours in central standard time. (Right) The upper-air time cross-section reveals that the steering flow changed from SW to W during a several-hour period when a major cyclone center moved north of Oklahoma City. The positions of the Cb symbols in the figure designate the heights of the steering levels. Note that a cloud makes a sharp right turn when it starts rotating and that it resumes a normal course when the rotation ceases.

south-southeast at 37 kt. The CAPPI echo boundaries at 5,000-ft. intervals between 5,000 and 50,000 ft. were drawn on two charts in order to separate the height contours into those visible from above and below. Thus the overhanging portions of the echo were contoured separately from the cloud-base topography. The term cloud base is thus used for that portion of the cloud visible from below.

An examination of figure 7 thus obtained reveals various characteristics of hook-echo circulation. The hole or the eye viewed from below tilts toward the major cell at levels below 50,000 ft. The tilt is estimated to be about 15° from the vertical. At levels up to about 15,000 ft., the CAPPI boundary of the major cell including the finger-like hook is very similar to that commonly observed. That is to say, the hook is pendant to the major cell at its rear right corner. As the height increases, the cloud overhangs appreciably into the right sectors obscuring the entire hook at levels above 25,000 ft. Above this level, a small eye is visible near the rear center of the major cell. Note that this feature is very similar to that of the May 26, 1963, case shown in figure 4.

The cloud-top contours give a view of the echo topography above the hook-echo circulation. The linear extrapolation of the semi-vertical axis of the hook-echo circulation penetrates the cloud top near the highest portion of the radar cloud above 50,000 ft. The small black circles with arrows attached represent this point. It should be noted that the shape of the CAPPI contour

at the 50,000-ft. level suggests that the turret top is being eroded by the strong north-northwesterlies overtaking the cloud top at this altitude.

3. TRANSLATIONAL MOTION

It has been known that the velocity of the thunderstorm cell accompanied by a hook echo is quite different from that of the ordinary cell which is not characterized by such a circulation. In the study of the Illinois tornadoes of April 9, 1953, Fujita [3] tracked non-rotating thunderstorm echoes in an effort to compare their direction of motion with those of a hook echo. It was found that the hook echo moved in a direction about 25° to the right from the direction of movement of other echoes located in the vicinity. Examination of the upper air soundings revealed that at no levels were the wind-direction angles larger than 250° while the tornado cyclone or the hook echo moved from a 270° direction.

A very similar result was obtained in the study of the May 26, 1963, case. Here, it was found that the direction of motion of an echo changed abruptly to the right as soon as the echo showed some evidence of rotation. The tracks of the echo during the afternoon are shown in figure 8. The black circles denote the positions of echoes with rotational characteristics. The short lines crossing the echo trajectories indicate the positions of echoes whose rotational characteristics could not be identified. It is of interest to see that the direction of echo motion

tends to return to its original course after rotation is no longer detectable. It is seen, however, that the final direction of movement loses its northerly component. Such differences in directions before and after the rotation may mean either a change in the large-scale wind field or the existence of a slow rotation which could not be detected by the pattern of PPI echoes.

The phenomenon of echo convergence in the vicinity of tornadoes was studied by Stout and Hiser [13] who pointed out that two echoes were in a collision course of about 30° directional convergence. A tornado formed at about the time and place where the edges of two echoes first met. The evidence of a right turn of the rotating cloud as presented in figure 8 indicates that a rotating echo and other non-rotating echoes which maintain the normal course appear to converge in the right sector. In the left sector, however, echo divergence takes place.

4. ECHO DIVERGENCE

It was pointed out in the previous section that non-rotating echoes to the right of the path of a rotating cloud tend to converge and those to the left, diverge. The effect of such divergence and convergence upon the echo intensity is worth discussing.

According to the study by Stout and Hiser [13] of the storm of May 28, 1954, two echoes first made contact at their boundaries and then merged. The intensity of the larger echo located to the north increased by 4 decibels about the time of merger, and heavy rain and hail occurred. Then a tornado developed southeast of the intense echo which took an abnormal course resulting in an echo convergence. It may be assumed, therefore, that a number of small echoes to the south of the rotating

cloud merge into the major storm cell which is characterized by some degree of rotational motion. The major cell will then intensify to a certain extent and produce heavy rain, hail, and/or tornadic storm.

Non-rotating echoes to the left of the rotating one diverge from the course of the latter. In other words, the distance between the rotating and non-rotating clouds increases, suggesting an increase in the volume between these clouds. The hydraulic analogy to this phenomenon is created by abruptly moving backward a small piston facing a wall. The liquid surface between the wall and the piston drops down as a result of the piston's motion and the space is filled up gradually to recover the original level. The initiation of gravitational waves is neglected in this analogy.

An actual case of such diverging echoes was observed on May 26, 1963. Figure 9 shows rather strong echoes in a north-south line at 1450 CST. Echoes E and G began rotation shortly before 1500 CST and changed their direction of motion from ENE to ESE, while the northernmost echo, A, kept moving ENE without changing its course and speed. Measurements revealed that the echo distance between A and E, which had been about 15 n. mi. until 1430 CST, increased to 21 n. mi. at 1500 CST, and to 33 n. mi. by 1530 CST. It is important to note that this relative motion or the relative displacement vector is in the direction perpendicular to that of the steering winds, and that the relative motion is as large as 20 n. mi. The divergence computed from the rate of increase in the area between the echoes is approximately 30×10^{-5} sec.$^{-1}$, which would create 10 ft. sec.$^{-1}$ of descending motion at the 30,000-ft. level unless a significant compensating flow is generated through the vertical north-south planes
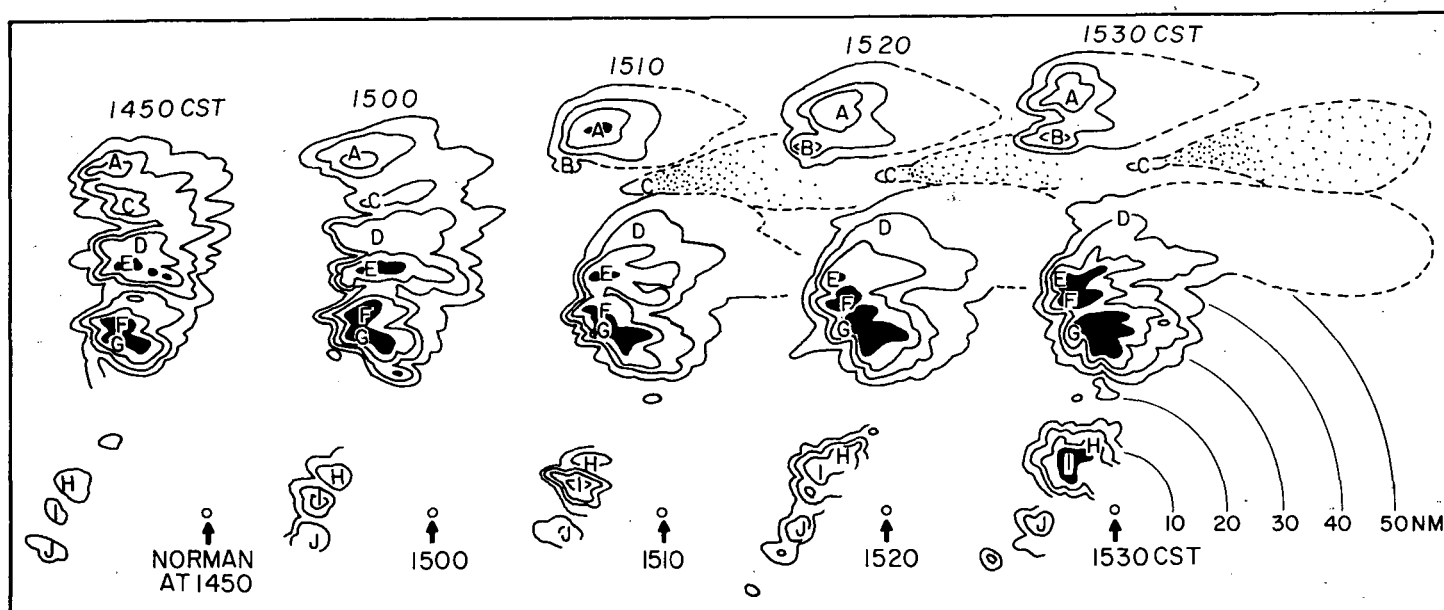

Figure 9.—Dissipation of the echo C caused by the sudden southward motion of the rotating echoes E and G. Analysis was made from the reduced-gain pictures taken by NSSL, Norman, Okla., on May 26, 1963. Elevation angle of the beam was approximately zero degree. The letters denote the same echoes which appeared in the previous figure. Analysis shows that echo E started rotating at 1440 CST when its course changed from ENE to SE, thus creating diverging space between echoes A and E.

limiting the east and west ends of the echoes. If we follow the echo C located between two large echoes, A and E, at 1450 CST, we see that it began to weaken 10 min. later when the echo E showed definite signs of rotation. The echo C at 1510 CST gives the impression that it turned into an anvil cloud pluming off from an extremely weak source.

5. PROPOSED MECHANISM OF HOOK-ECHO FORMATION

An updraft inside a thunderstorm provides an efficient means of collecting the underlying atmosphere into a small area at low levels in order to transport it upward. As a result, the updraft can be characterized by a significant rotation in the same sense as the absolute vorticity inside the underlying atmosphere. Under these favorable conditions, therefore, we may find a rotating updraft core characterized by a significant circulation, the sign of which may be either cyclonic or anticyclonic although the former dominates.

Now we consider that a rotating updraft with the circulation Γ is surrounded by a mass of cloud which is characterized by negligibly small circulation. The cloud as a whole will be steered by the horizontal winds within the layers up to the cloud top, although the momentum flux of the air continuously brought in from below and the falling hydrometeors complicate the problems extremely. The system involving the rotating updraft can, however, be simplified, as follows: (1) The central portion of a rotating updraft is more or less echo free because of inadequate time for the growth of cloud drops. This portion occasionally forms an eye on a PPI scope. (2) The eye-wall of the rotating updraft is characterized by echo-producing hydrometeors and a significant horizontal circulation superimposed upon strong vertical motions at low levels. (3) The outermost regions of the updraft are affected by the environmental wind field, the direction of which may vary with height. The vertical motion in this portion is rather weak.

According to the Magnus effect, later proved theoretically by Kutta-Joukowski, a solid cylinder rotating inside the perfect fluid, with a density ρ and a uniform flow speed of u, receives a force F toward the side of the highest resultant speed obtained by superimposing the rotational and translational speeds. This force is expressed by

$$F = \rho u \Gamma$$

where Γ denotes the circulation around the rotating cylinder which is imbedded inside a horizontal straight wind field. If the circulation is cyclonic, for which Γ is assumed positive, the force acting on the updraft, standing vertically inside a geostrophic straight flow, is proportional to the pressure gradient of the undisturbed uniform flow. When the sign of the circulation is changed to negative or anticyclonic, the direction of the force points toward the low-pressure side of the geostrophic flow.

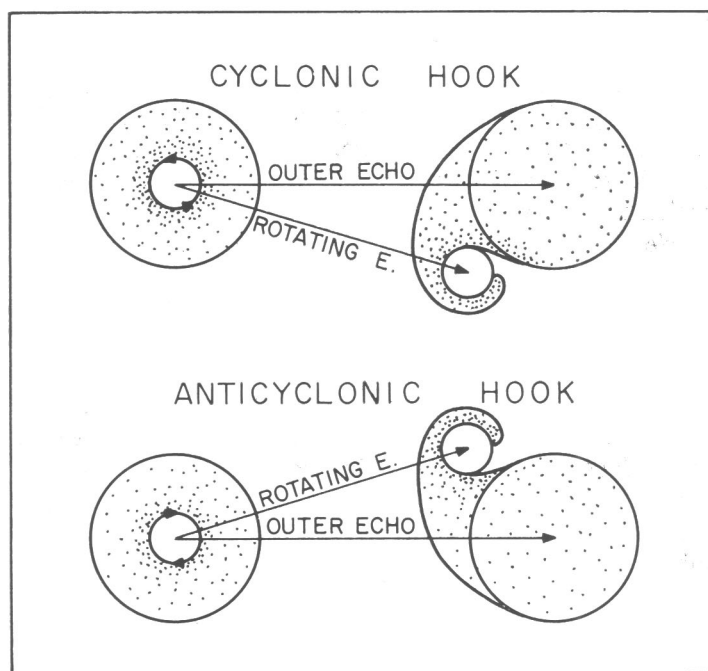A rotating cloud core is hardly a solid cylinder, but the

FIGURE 10.—Schematic diagram showing the position of the hook echo relative to the major cell moving west to east. The open circle at the center of the cloud to the left represents the eye surrounded by an eye-wall circulation. When this circulation moves out of the major echo a hook echo appears.
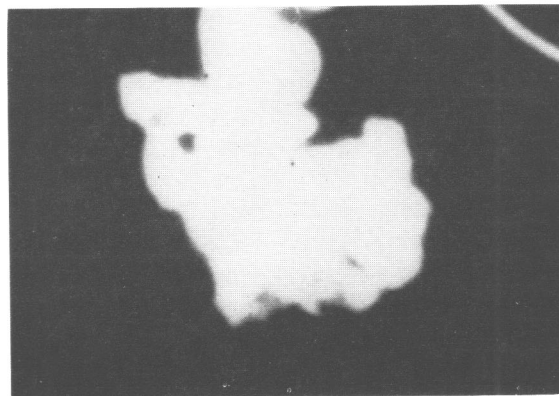

FIGURE 11.—An example of an anticyclonic hook of July 1, 1959. (From Fortner and Jordan [7].)

rising air in rotation is continuously supplied from low levels, thus permitting us to consider that it more or less acts as a mechanically-driven cylinder. Since the Magnus force is obtained by superimposing an irrotational vortex field around a cylinder upon a straight flow, it is necessary for the rotating cloud to induce a circulation around its immediate vicinity. Such a circulation will be induced by mixing a viscosity operating at various scales and lengths around the rotating cloud. The outer environment of the cloud is treated as a perfect fluid characterized by irrotational flow.

The schematic diagram of figure 10 represents the differential motions of the central and the outermost portions of clouds rotating either cyclonically or anti-

cyclonically. The figure shows that the echo surrounding the eye-wall moves more or less with the environmental winds, and much faster than the eye-wall consisting of the newly condensed hydrometeors. The outer portion has been exposed to the horizontal flow for some time and may have been diluted. This results in a situation in which the eye-wall will be left behind.

We may now expect the Magnus force to pull the spiraling updraft toward the high or low pressure side depending upon the sign of the rotation. As a result of this side pull the circulation center of the cloud ends up in the position indicated in figure 10. The lower figure, representing the anticyclonic hook, is extremely rare because most of the vigorous cumulonimbus convection takes place in the subcloud wind fields of absolute cyclonic vorticity. Presented in figure 11 is a rare example studied by Fortner and Jordan [7]. In this case the subcloud layer was dominated by an anticyclonic ridge extending inland from the Atlantic to Alabama where the anticyclonic hook occurred.

In this proposed mechanism of a hook-echo formation, one may observe an early stage of the circulation near the center of an intense updraft cell. This stage is schematically described in figure 12. As time passes, however, the separation of the surrounding and the central portions of the rotating updraft takes place through the movement of the eye toward the rear right end of the major cell, A B C E, which surrounded the rotating updraft in its formative stage.

At high levels the hook echo disappears and it takes the shape of a hole in the echo, because the spiraling updraft around the eye continuously generates condensed water droplets at such a rate that they are not eroded away within a short time. Near and above the anvil level, droplets and ice crystals spread out in all directions forming an anvil plume which can hardly be distinguished from that of a non-rotating cumulonimbus cloud of comparable size.

6. VORTICITY AND DIVERGENCE INSIDE TORNADO CYCLONES

Only a few measurements of the wind fields around tornado cyclones are available at present. Fujita's [4] computation showed that the tangential speed of the wall cloud of the Fargo storm with a diameter of 2.0 km. was 24 m.p.h. at the 2,000-ft. level, and the collar cloud, with a diameter of 4.4 km. located at the 4,000-ft. level, was rotating at the rate of 25 m.p.h. The circulation and mean vorticity computed from these values appear in table 1.

This table shows that the mean vorticity inside the wall cloud, which probably corresponds to the outer edge of the radar hook echo, is about $2,000\times10^{-5}$ sec.$^{-1}$. Outside the wall cloud, vorticity drops off considerably but circulation increases. Fujita [3] also computed the eastward speed of a small echo on the south edge of the hook of the Illinois tornado cyclone of April 9, 1953. It
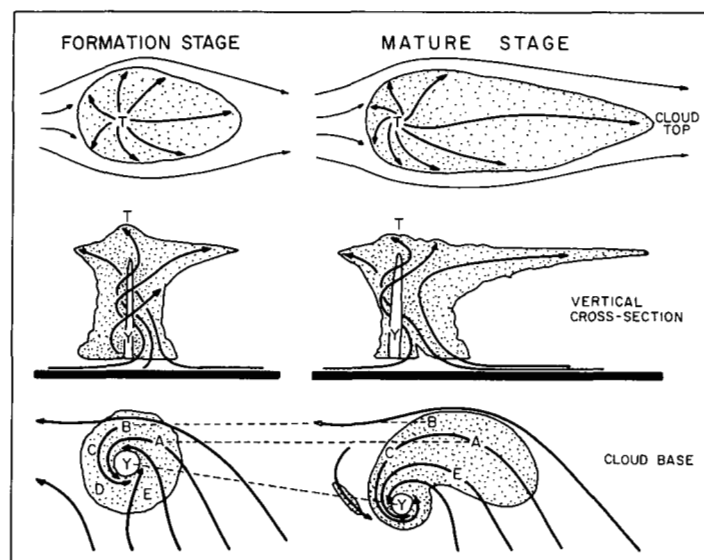

FIGURE 12.—A model of a rotating cumulonimbus. The formation stage takes place when a mature storm with an intense updraft moves over an area of pronounced low-level circulation which is commonly seen along a mesohigh boundary inside a major cyclone. As a result of the differential movement of the eye (Y) and the surrounding echo (A B C D E), we observe a hook pendant to a major thunderstorm cell in its mature stage.

was about 80 kt. while its center was translated eastward at the rate of 38 kt. These figures give the tangential speed of 42 kt. (20 m.p.s.) at a radius of 1.2 km. from the circulation center.

The convergence values beneath the rotating clouds can be computed either from the vector wind field or from the change in vertical motion with height. Since we have no data on the subcloud wind fields, an estimation of convergence will be made by this second method. A movie film showing the Fargo rotating cloud was used in calculating the vertical velocity as a function of height. The result was 70 ft. sec.$^{-1}$ at 3,000 ft. above the ground. Obtained from these figures is a mean convergence of $2,300\times10^{-5}$ sec.$^{-1}$, which is very similar in value to the mean vorticity.

It is reasonable to assume that the mean vertical motion of the spiraling updraft around the eye is over 1,000 ft. sec.$^{-1}$ which would carry the air from cloud base to the 40,000-ft. level in 6 or 7 min. On the other hand, the tangential speed of the air circling around the eye with a 2-km. radius is about 10 m.p.s., thus requiring about 20 min. for a parcel to complete one rotation around the

TABLE 1.—*Rotational characteristics of the Fargo tornado cyclone of June 20, 1957*

Radius (km.)	Tangential speed (m.p.s.)	Circulation ($\times10^5$ cm.^{2} sec.$^{-1}$)	Mean vorticity ($\times10^{-5}$ sec.$^{-1}$)
1.0	10	6	2,000
2.2	11	15	1,000
1.0 to 2.2			750

eye. This rotational and vertical motion combined does not permit any ascending parcel to rotate even once around the eye. Instead, the parcel seems to draw close to the cloud shortly after rotating 120° around the eyewall. The schematic diagram in figure 12 was constructed in the light of the above figures. Since a parcel inside the updraft does not complete even one rotation before reaching the anvil level, the axis of rotation may tilt from the local vertical. Up to about 20° tilt is usually observed in radar pictures showing the eye at various heights.

7. CIRCULATION AROUND TORNADOES

There is no direct measurement of the wind speed inside a tornado, since no anemometer has survived in the violent winds. Therefore, the best estimate must be made from indirect measurements.

In his elaborate calculation of the debris movement inside the Dallas tornadoes of April 2, 1957, Hoecker [9] estimated the highest tangential speed at the 225-ft. level to be 170 m.p.h. around the circle of 130-ft. radius. The vorticity within this circle is more or less constant, while the outer circulation is regarded as a vr vortex. The mean vorticity was found to be about $400,000 \times 10^{-5}$ sec.$^{-1}$ which is four times larger than that of the Fargo tornado computed from the funnel rotation. The circulation around the circle obtained from $2\pi r V_t$ is 1.9×10^8 cm.^{2} sec.$^{-1}$

An entirely different approach was made by Van Tassel [15] to compute the tangential wind speed. He examined the scratch marks left on a plowed field over which a tornado passed. The major and minor axes had dimensions of 230 ft. and 152 ft., respectively. The tangential speed of the tornadic circulation which left these scratch marks was computed to be 484 m.p.h. from the equation

$$V_t = CNS$$

where C denotes the circumference of the ellipse, N the number of scratch rings per mile, and S the translational speed of the tornado in m.p.h. The circulation around the tornado obtained from these figures would reach 3.0×10^8 cm.^{2} sec.$^{-1}$.

With the use of 16-mm. movie film of the Fargo tornadoes of June 20, 1957, Fujita [4] obtained the diameter and the tangential speed of the funnel cloud. The speed computed was only 48 m.p.s. at a radius of 110 m. from the funnel axis. The circulation corresponding to these values is 3.3×10^8 cm.^{2} sec.$^{-1}$ and the vorticity $90,000 \times 10^{-5}$ sec.$^{-1}$

TABLE 2.—*Circulation and vorticity around tornadoes*

Tornadoes	Tangential speed (m.p.h.)	Radius (ft.)	Circulation (×10³ cm.² sec.⁻¹)	Vorticity (×10⁻⁵ sec. ⁻¹)
Scottsbluff	484	76	3.0	1,900,000
Dallas	170	130	1.9	400,000
Fargo	108	360	3.3	90,000

759-602—65——2

These results are summarized in table 2. Although the number of storms available for these statistics is only three, the values are at least helpful in estimating the order of magnitude of the quantities involved. The circulation around these tornadoes, for instance, seems to be in the order of 10^8 cm.^{2} sec.$^{-1}$ while the other quantities vary considerably from storm to storm.

8. ABSOLUTE VORTICITY AND ABSOLUTE CIRCULATION

Although the present knowledge of tornado and tornado-cyclone circulation is not enough to discuss the dynamics and thermodynamics of the storm quantitatively, an attempt has been made to express the circulation characteristics of these storms and of much larger vortices commonly observed in the atmosphere.

First we express the absolute circulation and the absolute vorticity of circular vortices by

$$\Gamma_a = 2\pi r(V + r\omega \sin \phi) = 2\pi r V_a$$

and

$$Q_a = 2(V + r\omega \sin \phi)/r = 2V_a/r$$

where V_a represents the absolute tangential speed, which is the tangential speed, V, of a circulating parcel plus the rotational speed of the earth around the vortex center.

The logarithms of these quantities, written as

$$\log \Gamma_a = \log 2\pi + \log r + \log V_a$$

and

$$\log Q_a = \log 2 - \log r + \log V_a$$

indicate that the isolines of Γ_a and Q_a on a chart, log r vs log V_a, incline 45° to the coordinates and that they intersect each other at right angles. A chart on these coordinates including the isolines of Γ_a and Q_a is called the kinematic diagram. The absolute tangential speed expressed by

$$V_a = V + r\omega \sin \phi$$

is appreciably affected by the earth's rotation when the radius of the circulation is very large. The dashed lines labeled with the latitudes 15°, 30°, etc. represent the absolute tangential speed of the earth's rotation (fig. 13).

Various circulation systems expressed as a combination of Γ_a and Q_a were plotted in this diagram. It is of interest to find that the tornadoes, tornado cyclones, and large circulation systems, such as hurricanes and frontal cyclones, are located along a concave dashed line. This line runs in the direction of the conservation of absolute vorticity within the region of the macroscale circulations. For the tornadoes the direction is parallel to the isolines of absolute circulation. Between these two extremes are the tornado cyclones which produce tornadoes.
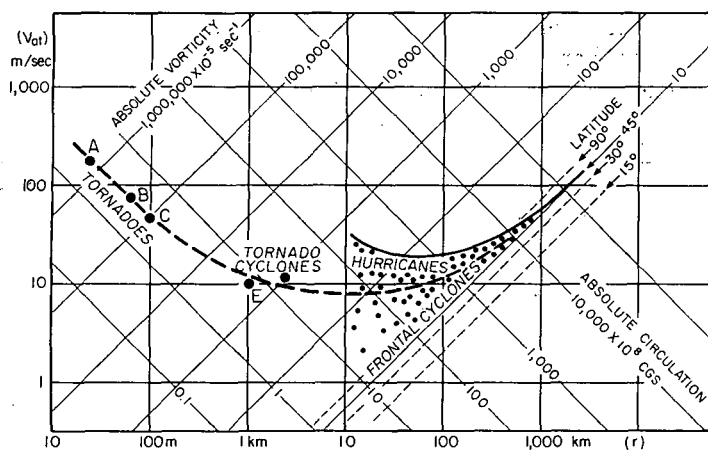
FIGURE 13.—A kinematic diagram of cyclonic circulation systems ranging from frontal cyclones to tornadoes. Storms identified are A, Scottsbluff Tornado (Van Tassel [15]); B, Dallas tornado (Hoecker [9]); C, Fargo tornado (Fujita [4]); and E, Fargo tornado cyclone (Fujita [4]).
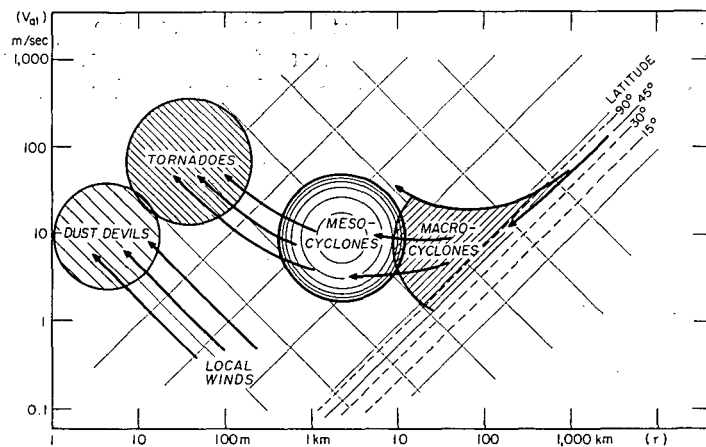

FIGURE 14.—A kinematic diagram showing possible changes in cyclonic wind systems of various horizontal dimensions. Only the systems at low levels are included in the diagram since no potential vorticity is computed for each system. In many cases, however, concentration of vorticity takes place within rather shallow layers above the surface when circulation regimes change under the influence of mesoscale convergence wind fields.

A further discussion of cyclonic systems, including tornadoes and dust devils, will be attempted with the use of the kinematic diagram shown in figure 14. It can be seen that a macroscale cyclone with a radius of several hundred kilometers is characterized by an absolute circulation of $1,000 \times 10^8$ cm.^{2} sec.$^{-1}$, which is 100 times larger than that of a tornado cyclone. It is, therefore, very unlikely that an entire macrocyclone converges into a tornado while maintaining its absolute circulation. Instead, a macroscale circulation breaks up into several mesocyclones before a part of it converges into a tornado circulation.

A PPI movie taken by the U.S. Weather Bureau's National Severe Storms Laboratory at Norman, Okla., on May 26, 1963, revealed an excellent example of such a breakdown of macroscale circulation into five mesocyclones (fig. 15). Each of these hook-echo circulations would produce a fair-sized tornado if, for some reason, the entire circulation were concentrated into a small area.

A mesoanalysis chart for 1700 CST, the time of the PPI photograph in figure 15, reveals that there existed a mesoscale high-pressure area with an elliptic boundary as indicated by the dashed line. It is of interest to find that the five hook echoes are located above the boundary, suggesting that a mesohigh boundary initiates favorable conditions giving rise to the development of vigorous thunderstorms with rotating updrafts. As proposed by Tepper [14], a pressure-jump line, commonly observed along the leading edge of a mesohigh, initiates tornadoes. The storms identified with numerals 3, 4, and 5 are seen at the locations postulated by Tepper's theory.

When we construct a mesosynoptic chart for 1700 CST (fig. 16), covering a much larger area than that of the PPI photograph, we see that the mesohigh was located near the center of a well-developed cyclone covering, at least, the entire State of Oklahoma. In fact the

mesohigh appeared at 1500 CST and quickly filled up the central region of the major cyclone. By performing a line integral of tangential wind speed along a closed circuit just inside this mesohigh boundary we obtain a circulation of about 5×10^5 m.^{2} sec.$^{-1}$ The cyclonic circulation along a closed circuit outside the mesohigh boundary is calculated to be about 10×10^5 m.^{2} sec.$^{-1}$, while the ring-shaped area between these two closed circuits is about 3×10^9 m.^{2} sec.$^{-1}$ The mean vorticity inside this ring-shaped area is thus estimated to be 50×10^{-5} sec.$^{-1}$ which is appreciably larger than that expected when there was no mesohigh. In other words, a mesohigh existing inside a large-scale cyclonic system creates a weak or strong anticyclonic vorticity near the cyclone center, and produces a narrow ring of intense cyclonic vorticity along the mesohigh boundary.

It should also be noted that the vorticity within this narrow ring along the mesohigh boundary is not distributed uniformly. In most cases, we observe intense vorticity along the progressing side of a mesohigh where southeasterly inflow and northwesterly outflow usually meet. Statistics reveal that this is the region where tornadoes form frequently. One example of tornado formation along the shear line is well described in the article by Ward [16] who observed the May 4, 1961, tornado in western Oklahoma. Through his observation he emphasized the importance of such a shear zone in the formation of tornadoes.

If a thunderstorm with weak updraft is located near a mesohigh boundary of this type, it would suck up only the warm air characterized by relatively small cyclonic vorticity. A giant thunderstorm with strong updraft will, on the other hand, suck up both warm and cold air located on both sides of the mesohigh boundary resulting in a concentration of cyclonic circulation integrated along
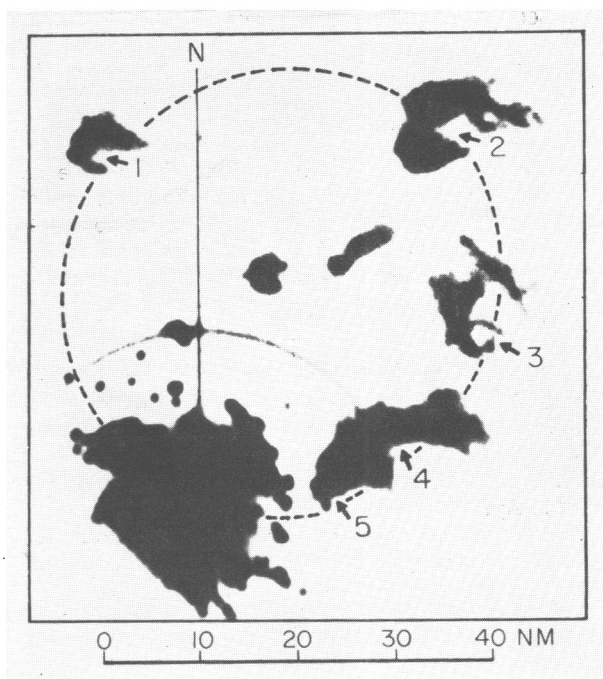
FIGURE 15.—Five mesocyclones appearing as hook echoes photographed by NSSL radar at Norman, Okla. on May 26, 1963. Time: 1700 CST. Antenna tilt: 0°.
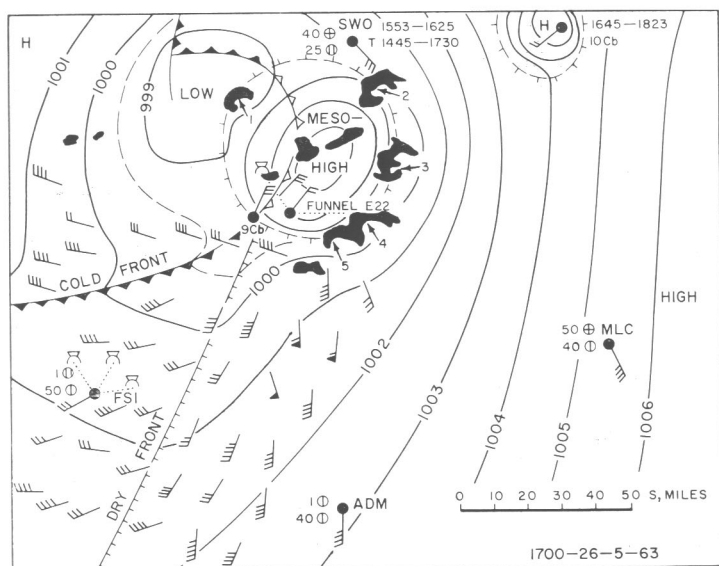

FIGURE 16.—Surface mesoanalysis chart for 1700 CST, May 26, 1963, when five hook echoes were photographed along a mesohigh boundary located near the center of a macroscale cyclone system. Radar picture of these echoes is shown in figure 15.

a circuit which crosses the boundary. It is well-known that an extremely low cloud base, something like a tail or a skirt, extends toward the source of the cold and high-humidity air which condenses at a very low level while moving into the base of a giant thunderstorm.

It may be postulated that a source of angular momentum necessary to initiate a rotating cloud or a hook echo is found along a mesohigh boundary existing within the field of a macroscale cyclonic circulation. A rare case, as shown in figure 16, was characterized by a significant

mesohigh located in the midst of a macrocyclone, thus setting off as many as five hook echoes around the mesohigh boundary.

Proposed 3-M Conditions. As the necessary conditions for the initiation of a rotating cloud, we may select the following: (1) *Macroscale cyclonic wind fields* at low levels, which provide basic vorticity of 20×10^{-5} sec.$^{-1}$ or more; (2) *Mesoscale high-pressure system* located inside the above system, which results in a concentration of significant cyclonic vorticity (50×10^{-5} sec.$^{-1}$ or more in average) along its boundary; and (3) *Major steady-state updraft* likely to develop under the influence of strong vertical wind shear.

These three conditions, *Macrolow*, *Mesohigh*, and *Major updraft* were found to have existed in the May 26, 1963, case when a family of rotating clouds appeared. There are a number of other cases of hook-echo formation in which these conditions were implicitly reported. A hurricane is a significant cyclonic wind system; however, its convective towers rarely show signs of rotation until the storm moves inland or over a relatively dry region where we expect to observe mesoscale high-pressure systems. Over tropical waters, the high humidity and the subsequent shallow subcloud layer prevent the development of cold domes over the surface. Thus the second condition is not satisfied inside a hurricane even though the first and third are predominant.

9. TORNADOES AND TORNADO CYCLONES

The kinematic diagram introduced in this paper represents the fact that the absolute circulation of a tornado is a few tenths of that of the tornado cyclones. Even if the entire vorticity at low levels beneath the mother circulation shrank into tornado funnels, it would be only enough to produce one or two tornado circulations.

The statistics of the Fargo tornadoes studied by Fujita [5] present several important facts. The path length of the tornadoes increases with the translational speed of the tornado cyclone; and the occurrence interval of a tornado family born from a tornado cyclone is 42 min. on the average, with very small standard deviation from storm to storm.

A tornado originating from a rotating cloud usually drops down in an oblique angle from the axis of the cloud circulation, and the tornado center on the ground is frequently located beneath the wall cloud to the right of the center when viewed in the direction of the translation vector of the mother circulation. An example of a view including a tornado and its mother cloud appears in figure 17. The tornado axis tilts in such a manner that its upward extension goes into the center of the rotating cloud. The angle is estimated to be about 30°. Numerous examples show that the tilt of a tornado axis is relatively small in the early stages of development through maturity. During the post-mature stage, the distance between the surface tornado and the mother cloud center increases and the axis displays a large tilt.

FIGURE 17.—Fargo tornado of June 20, 1957 extending down from a rotating cloud moving east. The picture was taken facing west from a distance of 5.4 mi. Exposure time: 1837 CST. Place: Dilworth, Minn. (Courtesy Mr. Littke.)

Because the absolute circulation of a tornado formed inside a tornado cyclone reaches a few tenths of that of the mother circulation, it seems that nature tends to avoid the production of more than one tornado simultaneously. However, there are numerous cases wherein a new tornado appeared while the old, dissipating one was still in sight.

10. CONCLUSIONS

This research suggests that a mechanism of the hook-echo formation is the differential translational motion of the rapidly rotating portion and the surrounding portion of a cloud. That is to say, the rotation originates near the heart of the cloud, then the rotational core moves differently from the rest of the cloud, thus forming the well-known pendant hook echo at low levels. At high levels, above 30,000 or 40,000 ft., however, the extension of the circulation axis is located beneath the dome of echo-top topography which is usually found near the center of the high-level echo. A hook echo which is observed to form near the rear right edge of a well-developed thunderstorm cell is simply an indicator of a pre-existing vortex which has moved out from a major echo. Such a vortex is sometimes strong enough to draw water droplets and other back-scattering particles out of the major cell.

A kinematic diagram with coordinates of absolute tangential speed vs. cyclone radius was made to relate physically the macro-, meso-, and micro-circulations. It has been shown that absolute circulation is likely to be conserved in micro-circulation, while absolute vorticity is conserved in macro-circulation. Mesoscale circulations existing in these two extremes are rather complicated since neither absolute vorticity nor circulation is conserved. The diagram also shows that only local winds, related to the local topography, and local heating are needed to produce dust devils. Waterspouts could also be produced locally without necessitating the existence of a mesoscale circulation to act as a mother circulation field.

REFERENCES

1. S. G. Bigler, "Observations of Tornado Using the AN/CPS-9 Radar," *Proceedings, Seventh Weather Radar Conference, Miami Beach, 1958,* American Meteorological Society, pp. K 1-5.
2. E. M. Brooks, "The Tornado Cyclone," *Weatherwise,* vol. 2, No. 2, April 1949, pp. 32-33.
3. T. Fujita, "Mesoanalysis of the Illinois Tornadoes of April 9, 1953," *Journal of Meteorology,* vol. 15, No. 3, June 1958, pp. 288-296.
4. T. Fujita, "A Detailed Analysis of the Fargo Tornadoes of June 20, 1957," *Research Paper* No. 42, U.S. Weather Bureau, Washington, D.C., 1960, 67 pp.
5. T. Fujita, "A Review of Researches on Analytical Mesometeorology," *Research Paper No. 8,* Mesometeorology Project, University of Chicago, 1962.
6. T. Fujita and J. E. Arnold, "Development of a Cumulonimbus Under the Influence of Strong Vertical Shear," *Proceedings, Tenth Weather Radar Conference, Washington, D. C., 1963,* American Meteorological Society, 1963.
7. L. E. Fortner, Jr. and C. L. Jordan, "A Non-Tornadic Spiral-Shaped Radar Echo," *Monthly Weather Review,* vol. 88, Nos. 9-12, Sept.-Dec. 1960, pp. 343-348.
8. J. R. Fulks, "On the Mechanics of the Tornado," *National Severe Storms Project Report* No. 4, U.S. Weather Bureau, 1962.
9. W. H. Hoecker, Jr., "Wind Speed and Air Flow Patterns in the Dallas Tornado of April 2 1957," *Monthly Weather Review,* vol. 88, Nos. 9-12, Sept.-Dec. 1960, pp. 167-180.
10. J. L. Marshall, "The Constant-Altitude Presentation of Radar Weather Patterns," *Proceedings, Sixth Weather Radar Conference, Cambridge, Mass., 1957,* American Meteorological Society, 1957, pp. 321-324.
11. S. Penn, C. Pierce, and J. K. McGuire, "The Squall Line and Massachusetts Tornadoes of June 9, 1953," *Bulletin of the American Meteorological Society,* vol. 36, No. 3, Mar. 1955, pp. 109-122.
12. G. E. Stout, and F. A. Huff, "Radar Records Illinois Tornadogenesis," *Bulletin of the American Meteorological Society,* vol. 34, No. 6, June 1953, pp. 281-284.
13. G. E. Stout and H. W. Hiser, "Radarscope Interpretations of Wind, Hail and Heavy Rain Storms between May 27 and June 8, 1954, *Bulletin of the American Meteorological Society,* vol. 36, No. 10, Dec. 1955, pp. 519-527.
14. M. Tepper, "A Proposed Mechanism of Squall Lines: The Pressure Jump Line," *Journal of Meteorology,* vol. 7, No. 1, Feb. 1950, pp. 21-29.
15. E. L. Van Tassel, "The North Platte Valley Tornado Outbreak of June 27, 1955," *Monthly Weather Review,* vol. 83, No. 11, Nov. 1955, pp. 255-264.
16. N. B. Ward, "Radar and Surface Observations of Tornadoes of May 4, 1961," *Proceedings, Ninth Weather Radar Conference, Kansas City, Mo., 1961,* American Meteorological Society, 1961, pp. 175-180.